

Magnetotransport properties of $\text{Nd}_2\text{Fe}_{14}\text{B}$

Jolanta Stankiewicz* and Juan Bartolomé

*Instituto de Ciencia de Materiales de Aragón, Consejo Superior de Investigaciones Científicas
and Universidad de Zaragoza, 50009-Zaragoza, Spain*

(Received 10 June 1998)

The electrical resistivity and Hall effect of a single crystal of $\text{Nd}_2\text{Fe}_{14}\text{B}$ have been measured over the temperature range of 10 to 300 K in magnetic fields of up to 12 T. At low temperature, a positive (both transverse and longitudinal) magnetoresistance is observed. It can be attributed to scattering of carriers by magnetization-dependent mechanisms. The magnetoresistance decreases strongly with increasing temperature as the suppression of spin fluctuations by an external field becomes more important. Hall resistivity data are holelike and follow the magnetization of the material. The low-field Hall resistivity peaks at about 130 K, in the vicinity of the spin-reorientation temperature in $\text{Nd}_2\text{Fe}_{14}\text{B}$. Away from the peak, the Hall resistivity is proportional to the square of the total resistivity. We find that both skew scattering and side-jump scattering contribute to the Hall effect. However, spin fluctuations are important only in a small region close to the spin-reorientation temperature whereas side-jump scattering governs the Hall effect in the whole temperature range studied. [S0163-1829(99)15501-2]

I. INTRODUCTION

Magnetic materials of the type $R_2\text{Fe}_{14}\text{B}$ (R =lanthanide series) are important for technological applications as permanent magnets. Since the discovery of $\text{Nd}_2\text{Fe}_{14}\text{B}$ in 1984,¹ these materials have been the subject of intensive research.²⁻⁴ Their strong uniaxial anisotropy, a large spontaneous magnetization, and a relatively high Curie temperature are attractive for applications, and their understanding poses an interesting challenge.

$\text{Nd}_2\text{Fe}_{14}\text{B}$ crystallizes in a tetragonal structure. Its unit cell, with 68 atoms, is quite complicated. Nd and Fe ions occupy two and six different crystallographic sites, with an average magnetic moment of 2.30 and of $2.1\mu_B$, respectively. Electronic band structure calculations show that the Fe d bands are most important in the density of states at the Fermi level although Nd $4f$ localized bands are found not far from it.⁵ The Fe sublattice provides most of the magnetization of $\text{Nd}_2\text{Fe}_{14}\text{B}$ while the magnetocrystalline anisotropy arises almost entirely from the Nd ions since they have nonvanishing orbital moments. Nd and Fe sublattice moments couple ferromagnetically; the Curie temperature is 586 K.⁶ At room temperature, the easy magnetization direction is the tetragonal c axis and the Nd and Fe sublattice moments are collinear. As the temperature decreases, $\text{Nd}_2\text{Fe}_{14}\text{B}$ exhibits a spin-reorientation transition.⁴ Below the spin-reorientation temperature, T_s ($T_s \approx 135$ K), the magnetization direction cants away from [001] towards the [110] direction, by an angle that increases with decreasing temperature, up approximately to 30° at 4 K. Features related to this transition have been found in nearly all sorts of measurements performed on $\text{Nd}_2\text{Fe}_{14}\text{B}$.⁴ The magnetic coupling strength between Nd and Fe moments is about half of the coupling strength between Fe ions. The Nd-Nd magnetic interaction is much weaker.⁴

In spite of the abundance of reports on the magnetic properties of $\text{Nd}_2\text{Fe}_{14}\text{B}$, there are only a few studies of its electron transport properties. One of them is a short report on the resistivity anomaly observed at the spin-reorientation transi-

tion temperature.⁷ Two other papers are devoted to the temperature dependence of the resistivity.^{8,9} It has been found that the low-temperature magnetic resistivity can be attributed to scattering of electrons by magnons and by spin fluctuations. The anomalous behavior of the resistivity just below the Curie temperature has been attributed to Invar-type coupling.

Electrical and magnetotransport properties are very sensitive to the electronic structure as well as to the magnetic nature of the materials studied. The magnetism of the inner $4f$ shell strongly affects the resistivity of rare-earth metals.¹¹ The s - f exchange interaction, which leads to the anomalous behavior of the conductivity in rare-earth materials,^{12,13} is also important in transport properties of intermetallic compounds with nontransition metals¹⁴ and of magnetic alloys.¹⁵ In particular, it may lead to anisotropy in magnetoresistance. Spin-orbit coupling, either intrinsic or extrinsic (arising from the s - d or s - f interaction), of magnetic electrons, gives rise to a magnetization-dependent Hall effect.¹⁶ The anomalous Hall resistivity can be a sensitive probe of the rearrangement of localized moments.¹⁷ Its magnitude has been shown to be proportional to the third moment of the magnetization fluctuations.^{18,19} Consequently, a strong enhancement of the anomalous Hall coefficient is expected close to magnetic phase-transition points. Such effects have been observed in pure ferromagnetic metals and in antiferromagnetic semiconductors.¹⁹ Intermetallic compounds with transition metals may show more complex behavior, $3d$ itinerant magnetism and $4f$ localized magnetic moments are present in them. The interplay between these two contributions is one of the most interesting features of $R_2\text{Fe}_{14}\text{B}$ compounds that is still not well understood. Magnetotransport measurements are very suitable for elucidating the role of each of these contributions. However, neither the magnetotransport properties of $\text{Nd}_2\text{Fe}_{14}\text{B}$ nor those of similar compounds have, to our knowledge, been studied.

In this paper we report results of electrical resistivity and Hall-effect measurements in $\text{Nd}_2\text{Fe}_{14}\text{B}$ single crystal in the

temperature range of 10–300 K and in magnetic fields of up to 12 T. A positive anisotropic magnetoresistance of about 6% is observed at lowest temperatures and highest magnetic fields applied. This effect decreases strongly with increasing temperature. Hall data for magnetic field applied along the [110] direction are holelike and follow the magnetization at least at 100 and 280 K. The low-field Hall resistivity peaks at about 130 K, in the vicinity of the spin-reorientation temperature in Nd₂Fe₁₄B. Away from the peak, the Hall resistivity scales with the square of the total resistivity. The results obtained enable us to determine the dominant mechanisms in the Hall effect and magnetoresistance. To the best of our knowledge, this is by far the largest transport effect ever observed that can be attributed to a spin-reorientation transition. The experimental procedure is described in Sec. II. Results of magnetoresistance and Hall-effect measurements are reported and discussed in Sec. III. Conclusions are drawn in Sec. IV.

II. EXPERIMENT

A single crystal of Nd₂Fe₁₄B used in our studies was grown by Sagawa by the floating-zone melting technique.⁶ The electrical resistivity and Hall-effect measurements were performed with a six-probe method on bar-shaped samples. The samples were spark cut from the bulk single crystal and had typical dimensions of $1 \times 1.5 \times 5$ mm³. Their crystallographic orientations were determined by x-ray diffraction. Before measurements, each sample was polished and checked for possible cracks. Contact leads were ultrasonically soldered to the samples. The specimens were mounted between two fixed copper plates on a sample holder to minimize thermal gradients and to avoid the effects of the large anisotropy torques on the samples when the external magnetic field was applied along the [110] and $[1\bar{1}0]$ directions. For measurements with the external magnetic field parallel to the easy magnetization direction, the specimen was left free to rotate. The relative error obtained for resistivity measurements is about 0.05%; absolute values were determined to within 5%. The temperature was determined to about 1 K at high temperatures and to about 0.2 K at low temperatures using chromel-alumel and chromel-AuFe thermocouples, respectively. In the presence of magnetic fields, the temperature was controlled using a calibrated carbon glass resistor. Magnetization measurements were performed on the same samples that were used in magnetotransport studies.

III. RESULTS AND DISCUSSION

Figure 1 shows how the zero-field resistivity, ρ , and the low-field Hall resistivity, ρ_H , of Nd₂Fe₁₄B vary with temperature in the range from 4 to 300 K. First, we discuss the temperature and magnetic-field dependence of the resistivity. At low temperatures, the measured resistivity approaches a small constant value. ρ increases rapidly with temperature from 50 to about 250 K. The corresponding increment amounts to approximately 60% of the total resistivity at 250 K. For higher temperatures, ρ increases more slowly. Such behavior resembles the temperature dependence of the resistivity found for R₂Fe₁₄B polycrystalline samples and can be analyzed in the same terms.⁹ Applying Matthiessen's rule,

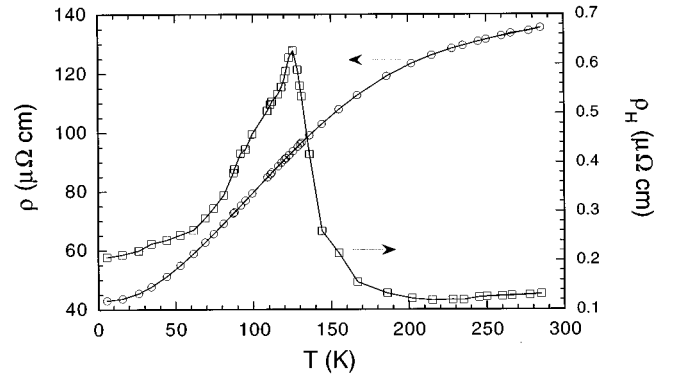


FIG. 1. Zero-field resistivity and low-field (0.1 T) Hall resistivity data points versus temperature of Nd₂Fe₁₄B single crystals. The solid lines are guides to the eye.

the total resistivity can be written as $\rho = \rho_0 + \rho_{ph} + \rho_{mag}$, where ρ_0 is the temperature independent residual resistivity, ρ_{ph} is the resistivity arising from electron-phonon scattering, and ρ_{mag} is the magnetic (spin) resistivity. At low-temperature ($T \lesssim 40$ K), $\rho_{mag} \propto T^2$. This behavior can be attributed to the scattering of electrons by magnons that involve mainly iron atoms. The scattering by mixed iron-rare-earth modes contributes less than 10% to the magnetic resistivity at low T , as estimated from the $\rho_{mag}(T)$ dependence. In the intermediate-temperature range, the carriers are scattered mainly by thermal spin disorder. We note that the value of the residual resistivity ($\rho_0 \cong 40 \mu\Omega \text{ cm}$) is quite high in our samples, probably because of large impurity concentration and static lattice imperfections.

The field dependence of the magnetoresistance of Nd₂Fe₁₄B is shown in Fig. 2 at various temperatures for different magnetic-field orientations. Current flow is always along the $[1\bar{1}0]$ direction. At 10 K, a positive (both transverse and longitudinal) magnetoresistance of about 6% is observed. An external magnetic field, \mathbf{H} , applied along the current direction, gives no classical magnetoresistance (no Lorentz force). Therefore, the observed rise of resistivity with H comes from the effect of magnetization. As can be gathered from Fig. 2, this contribution is slightly anisotropic, positive, and increases with increasing magnetic-field strength. This is contrary to the theoretical predictions for ferromagnetic metals, that suppression of spin fluctuations by an external field would lead to a negative magnetoresistance.¹⁰ We attribute most of the observed change of ρ with H to scattering mechanisms that depend on the magnetization, \mathbf{M} , namely skew and side-jump scattering.^{20,21} However, we estimate (see below) the contribution of side-jump scattering to magnetoresistance to be two orders of magnitude smaller than the measured value. Our data (see below) from Hall-effect measurements do not allow us to estimate the skew contribution. The difference between transverse and longitudinal magnetoresistances is shown in Fig. 3 as a function of magnetic field for two temperatures. This difference arises mainly from the classical magnetoresistance term that is proportional to H^2 . Assuming an electron mobility of about $5 \text{ cm}^2 \text{ V}^{-1} \text{ s}^{-1}$, the classical contribution should be about 1% of the zero-field ρ at low temperatures, which is close to the experimental value. The

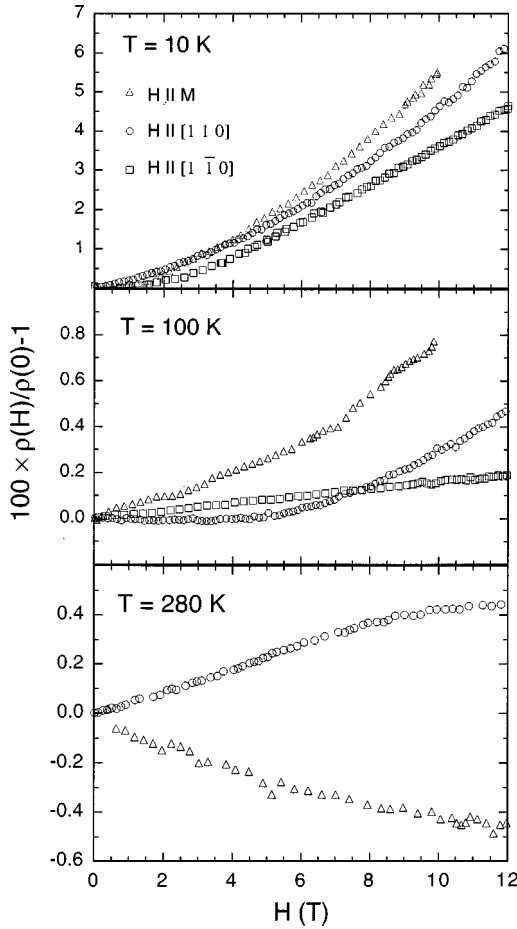


FIG. 2. Magnetoresistance of $\text{Nd}_2\text{Fe}_{14}\text{B}$ at various temperatures. The current flow direction is $[1\bar{1}0]$.

magnetoresistance of $\text{Nd}_2\text{Fe}_{14}\text{B}$ decreases rapidly as the temperature increases and turns slightly negative at room temperature for $\mathbf{H} \parallel \mathbf{M}$ (see Fig. 2). Scattering by spin fluctuations is more important at higher temperatures, and, therefore, their suppression by an applied magnetic field becomes more evident in magnetoresistance.

We now turn to the discussion of our Hall-effect data. Figure 4 shows how the Hall resistivity of $\text{Nd}_2\text{Fe}_{14}\text{B}$ varies with applied magnetic field at three different temperatures.

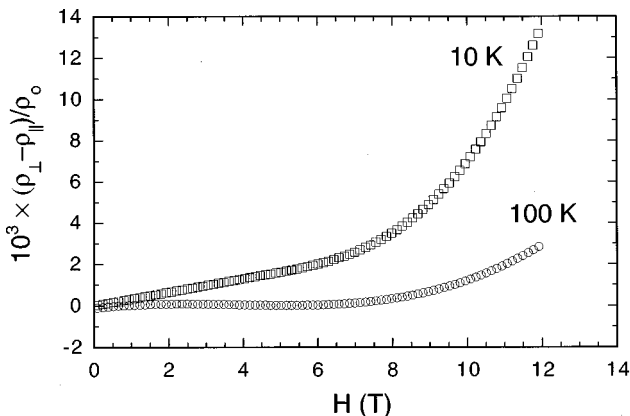


FIG. 3. The difference between perpendicular ($\mathbf{H} \parallel \mathbf{I}$) and longitudinal ($\mathbf{H} \parallel \mathbf{M}$) resistivity, normalized to the zero-field value, as a function of the external magnetic field.

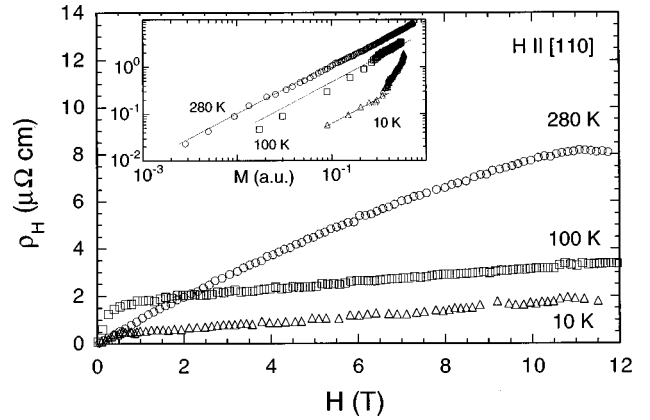


FIG. 4. The Hall resistivity as a function of magnetic field of $\text{Nd}_2\text{Fe}_{14}\text{B}$ single crystals for three different temperatures. The inset shows the same data as a function of magnetization.

At 10 and 100 K, ρ_H rises sharply up to approximately 0.2 T; it increases more slowly and almost linearly with field thereafter. At 280 K, ρ_H increases with field up to 11 T, where it starts to decrease slightly. The same data are plotted as a function of magnetization in the inset of Fig. 4. [The magnetization has been measured on the same samples that have been used in electrical transport measurements in a field of up to 5 T. The $M(H)$ dependence for higher fields has been extrapolated from the data in Ref. 22.] It is clear that the Hall resistivity data, which are holelike, follow the magnetization of the sample, at least at two (100 and 280 K) of the three temperatures for which measurements were made. The low-field Hall resistivity is shown in Fig. 1. It passes through a sharp maximum near 130 K; away from the maximum, ρ_H increases with increasing temperature.

Phenomenologically, the Hall resistivity is defined by

$$\rho_H = R_0 \mathbf{B} + R_s 4 \pi \mathbf{M} = R_0 [\mathbf{H} + 4 \pi \mathbf{M} (1 - N)] + R_s 4 \pi \mathbf{M}, \quad (1)$$

where R_0 is the ordinary Hall coefficient, R_s is the spontaneous Hall-effect (SHE) coefficient (also called anomalous), \mathbf{B} is the applied magnetic induction, \mathbf{M} is the spontaneous magnetization, and N is the demagnetization factor. Usually, the R_s is much larger than R_0 in magnetic samples. This is also true for our samples. At $T = 280$ K, a saturation, followed by a very slight decrease, of the Hall resistivity with field is observed. If we ascribe this change to the ordinary Hall effect, we obtain $R_0 \cong -2 \times 10^{-4} \text{ cm}^3 \text{C}^{-1}$ and a rough estimate of the electron concentration as $3 \times 10^{22} \text{ cm}^{-3}$. SHE in ferromagnetic materials has been the subject of many publications since the seminal work of Karplus and Luttinger in 1954.²³ It has been shown that various mechanisms contribute to it. One of them, skew scattering, arises from asymmetric scattering by impurities or phonons, and can be accounted for with a classical Boltzmann equation. It is brought about by spin-orbit coupling and is characterized by a constant spontaneous Hall angle: $\theta_H = \rho_H / \rho$, by which angle the scattered carriers deviate from their original trajectories.^{20,24} Another effect, a constant lateral displacement Δy (side-jump) of the charge carrier's trajectory at every scattering event, either by impurities or by phonons, is nonclassical and is also related to the spin-orbit interaction.²¹

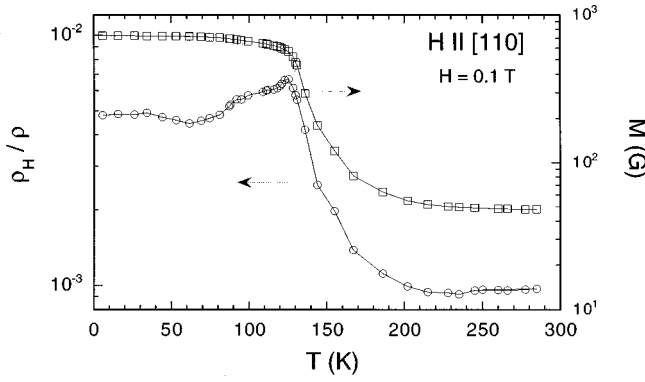


FIG. 5. Hall angle and magnetization at $H=0.1$ T, as a function of temperature, for Nd₂Fe₁₄B.

For this mechanism, $\theta_H \propto \rho$. A simple relation is satisfied between the SHE and the longitudinal resistivity:²⁵

$$R_s = a\rho + b\rho^2, \quad (2)$$

where the first term stands for the skew component, and the second term gives the side-jump contribution to the anomalous Hall coefficient. Dilute impurities and spin disorder are expected to give $R_s \propto \rho$, whereas phonons and concentrated spin defects lead to $R_s \propto \rho^2$. Consequently, SHE is usually attributed to skew scattering when ρ is small, and to side-jump scattering when ρ is large, e.g., in concentrated or disordered materials. We obtain the values of the SHE coefficient from: $R_s = \rho_H/4\pi M$, where ρ_H is the low-field Hall resistivity (shown in Fig. 1) and M is the value of magnetization measured with the same field (0.1 T) applied to the same sample. The temperature variations of the low-field Hall angle and of the magnetization are shown in Fig. 5. It is remarkable that both quantities rise sharply upon cooling, near the spin-reorientation temperature. The signature of this transition is also seen in the anomalous Hall coefficient, shown by open squares in Fig. 6. It appears as a dip in the $R_s(T)[R_s(\rho)]$ curve since ρ_H decreases with T more rapidly than M does in the vicinity of T_s . We fit our experimental results for Nd₂Fe₁₄B to Eq. (2), but with the skew scattering term modified, following the results of Kondo and

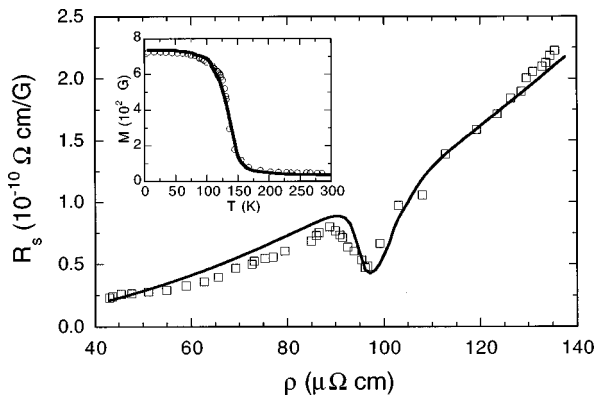


FIG. 6. Anomalous Hall coefficient, $R_s = \rho_H/4\pi M$, as function of the total resistivity for Nd₂Fe₁₄B single crystals. The solid line is a fit to experimental points. Experimental (open circles) and calculated (solid line) magnetization as a function of temperature are shown in the inset.

Maranzana.^{18,19} Considering the interaction between localized spin and conduction-electron orbital momentum, they have shown that the anomalous resistivity is proportional to the third moment of the magnetization fluctuations: $\rho_H \propto M_3$, where $M_3(T) = \langle (M - \langle M \rangle)^3 \rangle$. We have calculated M_3 for Nd₂Fe₁₄B within a phenomenological model for an anisotropic ferromagnet.²⁶ In this model, for \mathbf{H} in the [110] direction, the total magnetic energy is equal to

$$E = K_1 \sin^2 \theta + \tilde{K}_2 \sin^4 \theta + \tilde{K}_3 \sin^6 \theta - HM_s \sin \theta, \quad (3)$$

where θ is the angle between the c axis and the magnetization vector, M_s is the saturation magnetization, and $K_1, \tilde{K}_2, \tilde{K}_3$ are uniaxial anisotropy constants.²⁶ From the equilibrium condition, $dE/d\theta=0$, from which $M(H, T)$ follows. Values for $M_s(T), K_1(T), \tilde{K}_2(T), \tilde{K}_3(T)$ have been reported by several authors.^{22,26} The anisotropy constant values they give have been determined from the variation of M with respect to H between 0 and 20 T for different temperatures. We happen to be interested in the values of these constants near 0.1 T. The anisotropy constant values reported do not give a very good fit of M versus T at such low values of H . We find that a slight change (within 3%) in the value of K_1 given by Bolzoni²⁶ leads to a significant improvement of this fit. We use the ‘‘corrected’’ anisotropy constant values throughout this paper. The calculated magnetization is shown by a solid line in the inset of Fig. 6. Agreement with experiment is fairly good. The spin-moment fluctuations have been obtained by taking the second derivative (numerically) of the magnetization with respect to the magnetic field. The best fit to the spontaneous Hall coefficient ($R_s = aM_3/4\pi M + b\rho^2$), shown in Fig. 6, yields $a = 4 \times 10^{32} \Omega \text{ cm}^{-5}$ and $b = 0.0115 \Omega^{-1} \text{ cm}^{-1} \text{ G}^{-1}$. These values are in good agreement with theoretical predictions. Maranzana gives for the prefactor a the following expression: $a = (3N/2V)(\sin k_F d/E_F d)(g/\hbar)J^2$, where E_F and k_F are the Fermi energy and wave vector, respectively; d is the lattice constant; J and g are an exchange constant and the Landé splitting factor, respectively.¹⁹ Assuming $(N/V) \cong 3 \times 10^{22} \text{ cm}^{-3}$, $J = 5 \text{ meV}$, $E_F = 3 \text{ eV}$, and $d = 3 \times 10^{-8} \text{ cm}$,^{4,21} one obtains $a = 3 \times 10^{32} \Omega \text{ cm}^{-5}$, which is only 30% smaller than the value we have obtained. This is surprising considering how rough our approximations are. On the other hand, Berger has shown that $b = \gamma_{Hs}/4\pi M_s$, where $\gamma_{Hs} = ne^2 \Delta y/\hbar k$.²¹ For the same parameter values as above and for, following Ref. 21, $\Delta y = 1.5 \times 10^{-9} \text{ cm}$, we obtain $b \cong 0.011 \Omega^{-1} \text{ cm}^{-1} \text{ G}^{-1}$, which is very close to our result.

Therefore, a combination of skew and side-jump scattering explains our experimental results for SHE in Nd₂Fe₁₄B. Scattering by spin fluctuations is only effective in a narrow temperature region near the spin-reorientation temperature. Magnetization fluctuations are large in this region as Fe and Nd magnetic moments cant away from the collinear orientation to a noncollinear arrangement.²⁷ Our results point out the importance of the localized spin-charge-carrier interaction therein. Away from the spin-reorientation region, SHE appears to follow from side-jump scattering rather than from skew scattering. This is reasonable since the residual resistivity is high in our samples. The length of the side jump, which can be independently obtained from the Hall angle

variation with magnetization, amounts to 2×10^{-9} cm, which is very close to the one-band estimate in ferromagnetic materials.²¹

IV. CONCLUDING REMARKS

We have measured the resistivity and Hall effect of a Nd₂Fe₁₄B single crystal as a function of temperature and magnetic field. It turns out that the low-temperature behavior of its magnetoresistance can be attributed to scattering of electrons by mechanisms dependent on the magnetization. However, the contribution from side-jump scattering to magnetoresistance,²¹ which, for low fields, is given by $\Delta\rho/\rho = H(M/M_s)(e\Delta y/\hbar k_F) \cong 10^{-9}H(\text{G})$, is too small to explain our results. It would be helpful to study the high-field limit behavior of ρ in our samples. Unfortunately, it would require magnetic fields of the order of 10^4 T, which are difficult to reach experimentally.

The low-field Hall resistivity passes through a sharp maximum in the vicinity of the spin-reorientation tempera-

ture. This is the largest electronic transport effect we know about that can be attributed to a spin reorientation. We should note that we do not find any resistivity anomaly at the spin-reorientation transition. Magnetization fluctuations affect resistivity much less than the SHE. This effect is proportional to the second moment of the magnetization which does not vary as sharply through the transition as M_3 does. In addition, scattering mechanisms that are magnetization independent, such as scattering by impurities or static lattice defects, seem to be important in our samples. Obviously, they mask magnetization-dependent effects.

ACKNOWLEDGMENTS

We are indebted to Dr. Jesús Chaboy for comments on the manuscript and to Dr. Pedro Martinez for his continued assistance with computer work. This work was supported by Project MAT 96-448 of Comisión Interministerial de Ciencia y Tecnología (CICYT).

*Electronic address: jolanta@posta.unizar.es

¹M. Sagawa, S. Fujimura, N. Togawa, H. Yamamota, and Y. Matsuura, *J. Appl. Phys.* **55**, 2083 (1984).

²K. H. J. Buschow, in *Ferromagnetic Materials, A Handbook on the Properties of Magnetically Ordered Substances*, edited by E. P. Wohlfarth and K. H. J. Buschow (North-Holland, Amsterdam, 1988), Vol. 4, p. 1.

³E. Burzo and H. R. Kirchmayr, in *Handbook on the Physics and Chemistry of Rare Earths*, edited by K. A. Gschneidner and L. Eyring (Elsevier Science, Amsterdam, 1989), Vol. 12, p. 71.

⁴See J. F. Herbst, *Rev. Mod. Phys.* **63**, 819 (1991), and references therein.

⁵W. Y. Ching and Zong-Quan Gu, *J. Appl. Phys.* **61**, 3718 (1987); K. Hummler and M. Fähnle, *Phys. Rev. B* **53**, 3290 (1996).

⁶S. Hirosawa, Y. Matsuura, H. Yamamoto, S. Fujimura, M. Sagawa, and H. Yamauchi, *J. Appl. Phys.* **59**, 873 (1986).

⁷F. J. Lazaro, J. Bartolomé, R. Navarro, C. Rillo, F. Lera, L. M. Garcia, J. Chaboy, C. Pique, R. Burriel, D. Fruchart, and S. Miraglia, *J. Magn. Magn. Mater.* **83**, 289 (1990).

⁸J. B. Sousa, M. M. Amado, R. P. Pinto, V. S. Amaral, and M. E. Braga, *J. Phys.: Condens. Matter* **2**, 7543 (1990); J. B. Sousa, M. M. Amado, R. P. Pinto, M. A. Salgueiro, M. E. Braga, and K. H. J. Buschow, *ibid.* **3**, 4119 (1991).

⁹J. Stankiewicz and J. Bartolomé, *Phys. Rev. B* **55**, 3058 (1997).

¹⁰K. A. McEwen, *Handbook on the Physics and Chemistry of Rare Earths*, edited by K. A. Gschneidner and L. Eyring (North-Holland, Amsterdam, 1978), Vol. 1, p. 469.

¹¹B. Coqblin, *The Electronic Structure of Rare-Earth Metals and Alloys: The Magnetic Heavy Rare-Earth* (Academic, London, 1977).

¹²T. Kasuya, *Prog. Theor. Phys.* **16**, 58 (1956).

¹³P. G. de Gennes and J. Friedel, *J. Phys. Chem. Solids* **4**, 71 (1958).

¹⁴E. Gratz and M. J. Zuckermann, in *Handbook on the Physics and Chemistry of Rare Earths*, edited by K. A. Gschneidner and L. Eyring (North-Holland, Amsterdam, 1982), Vol. 5, p. 117.

¹⁵A. Fert, *Physica (Amsterdam)* **86-88B**, 491 (1977).

¹⁶C. M. Hurd, *Contemp. Phys.* **16**, 517 (1975).

¹⁷S. P. McAlister and C. M. Hurd, *Phys. Rev. Lett.* **37**, 1017 (1976).

¹⁸J. Kondo, *Prog. Theor. Phys.* **27**, 772 (1962).

¹⁹F. E. Maranzana, *Phys. Rev.* **160**, 421 (1967).

²⁰L. Berger, *Phys. Rev.* **177**, 790 (1969).

²¹L. Berger, *Phys. Rev. B* **2**, 4559 (1970).

²²Li Hong-Shou, Ph.D. thesis, L'Université Scientifique et Médicale et L'Institut National Polytechnique de Grenoble, 1987.

²³R. Karplus and J. M. Luttinger, *Phys. Rev.* **95**, 1154 (1954).

²⁴J. Smit, *Physica (Amsterdam)* **21**, 877 (1955).

²⁵J. M. Luttinger, *Phys. Rev.* **112**, 739 (1958).

²⁶F. Bolzoni, O. Moze, and L. Paretì, *J. Appl. Phys.* **62**, 615 (1987).

²⁷J. Chaboy, L. M. García, F. Bartolomé, A. Marcelli, G. Cibin, H. Maruyama, S. Pizzini, A. Rogalev, J. B. Goedkoop, and J. Goulon, *Phys. Rev. B* **57**, 8424 (1998).